

Pulsed and continuous wave solid phase laser annealing of electrodeposited CuInSe_2 thin films

Ashish Bhatia^{*a}, Helen Meadows^b, Alexandre Crossay^b, Phillip J. Dale^b, Michael A. Scarpulla^{a,c}

^aMaterials Science and Engineering, University of Utah, 122 S Central Campus Drive, Salt Lake City, UT, USA 84112; ^bLaboratoire Photovoltaïque, University of Luxembourg, 41, rue du Brill, L-4422 Belvaux, Luxembourg; ^cElectrical and Computer Engineering, University of Utah, 50 S Central Campus Drive, Salt Lake City, UT, USA 84112

ABSTRACT

Cu(In,Ga)Se_2 (CIGS) thin film photovoltaic absorber layers are primarily synthesized by vacuum based techniques at industrial scale. In this work, we investigate non-vacuum film synthesis by electrochemical deposition coupled with pulsed laser annealing (PLA) and or continuous wave laser annealing (CWLA) using 1064 nm laser. PLA results indicate that at high fluence ($\geq 100 \text{ mJ/cm}^2$) CuInSe_2 films melt and dewet on both Mo and Cu substrates. In the submelt PLA regime ($\leq 70 \text{ mJ/cm}^2$) no change in XRD results is recorded. However CWLA at 50 W/cm^2 for up to 45 s does not result in melting or dewetting of the film. XRD and Raman data indicate more than 80% reduction in full width at half maximum (FWHM) in their respective main peaks for annealing time of 15 s or more. No other secondary phases are observed in XRD or Raman spectrum. These results might help us in setting up the foundation for processing CIGS through an entirely non-vacuum process.

Keywords: Cu(In,Ga)Se_2 , pulsed laser annealing, continuous wave laser annealing

1. INTRODUCTION

Cu(In,Ga)Se_2 (commonly denoted as CIGS but more logically as CIGSe) has the tetragonal chalcopyrite structure and offers a number of desirable properties for use in solar cells. For example it is a direct band gap ($\approx 1 \text{ eV}$) material with the highest optical absorption coefficient ($\alpha \approx 10^5 \text{ cm}^{-1}$) amongst known inorganic semiconductors, a low surface recombination velocity etc. Over the years CIGSe technology has emerged from the laboratory with industrial module efficiency reaching close to 16% [1] and champion cells exceeding 20% [2]. In principle an ideal processing method for large scale production of CIGSe would be fast, cost-effective, reliable, scalable, and not energy intensive all while producing high-efficiency solar cells. Keeping this in mind we have tried synthesizing device quality CIGSe material from an entirely non-vacuum process by coupling electrochemical deposition with pulsed laser annealing (PLA) and or continuous wave laser annealing (CWLA).

In electrochemical deposition, ions in the solution are assembled as atoms on the surface of the back contact to form a semiconductor precursor thin film by the application of a modest voltage. Compared to vacuum deposition, electrochemical deposition has the advantages of requiring only a small amount of energy, allowing fast deposition rates $\sim 20 \text{ }\mu\text{m/hr}$ [3], and effective material utilization. Recently, Solopower Inc. has scaled up the electrodeposition of CIGS for manufacturing. [4] Despite the advantages offered by electrochemical deposition, as-electrodeposited (ED) thin film semiconductors are not useful in devices without thermal annealing to form the desired semiconductor phase, to improve crystallinity, and to minimize structural and electronic defects. [5]

Laser annealing on the other hand is quite different from the conventional furnace annealing (FA) and or rapid thermal annealing (RTA). The main advantage that laser annealing offers over the FA and or RTA is selective heating of the sample i.e. one can heat the active absorber layer without heating the substrate by choosing the correct wavelength of the laser beam. The absorption coefficient (α) of the material determines the absorption depth of the photons based on their wavelength (energy). In general longer wavelength (higher energy) photons will be absorbed much deeper in the material followed by (loosely speaking) heat generation and propagation. [6] Today lasers are being used for selective emitter doping of c-Si cells and line beams up to 750 mm wide are available for thin Si recrystallization for display technologies.

We have earlier reported results on PLA of electrodeposited CuInSe₂ thin films [7-8] using a 248 nm excimer laser. Although we saw improvements in crystalline quality of the samples by X-ray diffraction (XRD) and electron back scatter diffraction (EBSD), the CuInSe₂ films dewetted on both Mo and MoSe₂ substrates and hence were not useful for photovoltaic applications. We also note that careful inspection of the scanning electron micrographs in Ref. [9] reveal similar problems with dewetting which would also render such films useless for thin film photovoltaic absorber layers. In this work we report on CuInSe₂ laser processing using 1064 nm laser which has a longer absorption depth (~ 500 nm) as compared to 248 nm laser (~ 10 nm) thus ensuring more uniform heating through the film. There has also been some work reported by different groups [10-13] with little or no success for processing CuInSe₂ using laser both in pulsed and or CW modes, however more work needs to be done in order to understand laser annealing of CuInSe₂ and its effects on the optoelectronic quality of resulting CuInSe₂ layers.

2. EXPERIMENTAL DETAILS

2.1 Sample synthesis and preparation

The overall procedure to deposit CuInSe₂ thin films was similar to Ref. [5]. However the main difference was in the concentration of salts used, which is 4.33 mM CuSO₄, 12.8 mM InCl₃, 7.33 mM H₂SeO₃ and 160 mM LiCl. The deposition was carried out for approximately 25 minutes which gave a thickness of around 600 nm to the samples. The as-ED 1” x 1” CuInSe₂ films were then cleaved into ~ 6 mm x 6 mm samples. PLA and CWLA was done using a solid state Nd:YAG (neodymium-doped yttrium aluminum garnet) laser ($\lambda = 1064$ nm). In case of PLA the pulse width is ~ 75 ns. Figure 1 shows the setup of our laser system. The use of 1064 nm laser, as described earlier ensured deeper penetration of photons and uniform heating of the absorber layer. From the different experiments conducted on various samples we decided to work with a photon flux of 50 W/cm² and have varied the annealing time from 15 s to 45 s. Since the size of laser spot is 2 mm x 2 mm, a micrometer controlled X-Y stage was used to anneal the full area of the samples i.e. ~ 6 mm x 6 mm. During the course of annealing, samples were held in a customized annealing chamber, having quartz window at the top. The annealing chamber was purged with flowing Ar gas to provide an inert atmosphere and suppress oxidation.

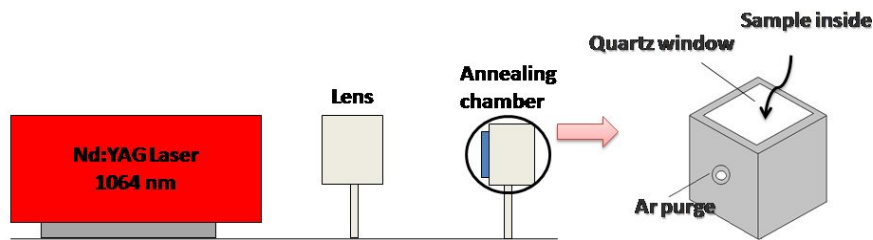


Figure 1. Schematic of our laser annealing setup and annealing chamber.

2.2 Characterization

X-ray diffraction (XRD) measurements (θ - 2θ) were carried out at 45 kV and 40 mA excitation using CuK α radiation in a range varying from $2\theta = 20^\circ$ - 60° . Scanning electron microscopy (SEM) was used to investigate the surface morphology and energy dispersive x-ray (EDS) analysis to determine the bulk composition of the samples was done at an acceleration voltage of 15 kV. Raman spectra were recorded using a micro-Raman spectrometer with 532 nm laser excitation at room temperature.

3. RESULTS AND DISCUSSION

3.1 Pulsed laser annealing (PLA) using 1064 nm laser

Figure 2(a) shows the SEM image of as-ED_ref sample. The surface morphology of as-ED sample appeared to be quite rough with RMS roughness value of > 200 nm. [8] Since liquid phase annealing is expected to give larger grain size we first attempted to anneal CuInSe₂ films via high temperature liquid phase annealing ($T > T_{\text{melt}}$) using 1064 nm PLA. However since liquid phase CuInSe₂ dewets on Mo and MoSe₂[7-8], an attempt was made to avoid dewetting via depositing CuInSe₂ films on Cu substrate. Fig.2(b) shows the result of PLA sample at 100 mJ/cm² after 5 laser pulses at 10 Hz. For comparison SEM image of a similar CuInSe₂ film on Mo annealed under same conditions is shown in Fig.2(c). As can be seen from the Fig., 2(b) unfortunately changing the substrate to Cu also did not help in prevention of dewetting.

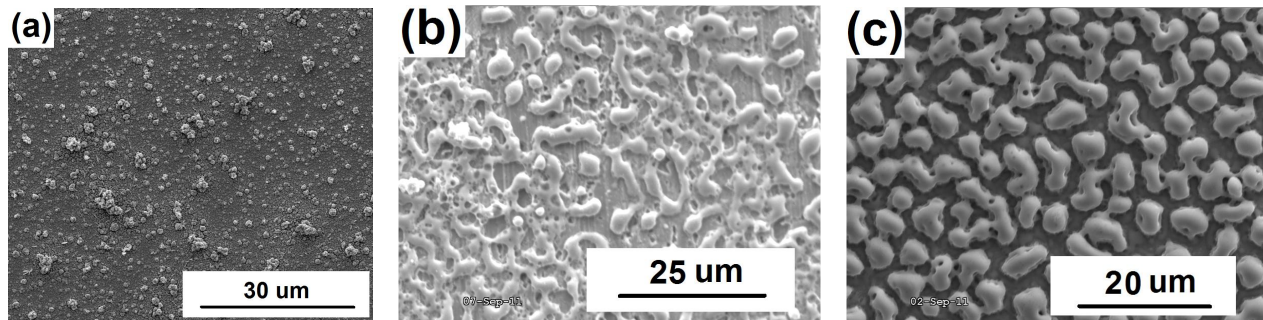
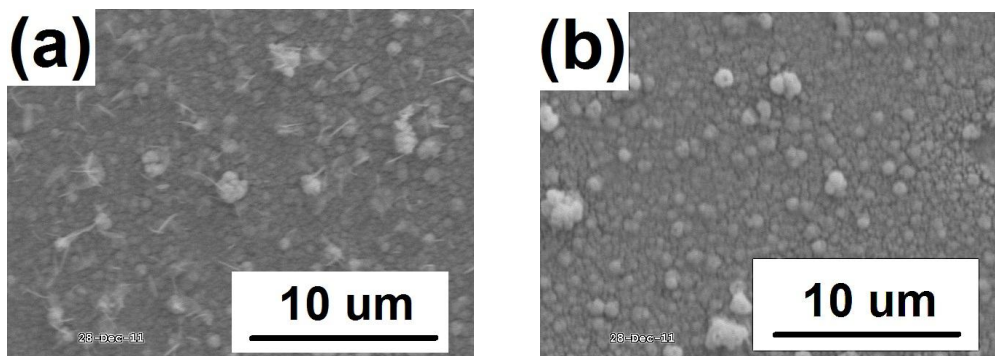


Figure 2. SEM images of (a) as-ED_ref CuInSe₂ film, and (b) and (c) show as-ED CuInSe₂ film after PLA at 100 mJ/cm² using 1064 nm laser deposited on Cu and Mo substrate. The SEM images shown are at 2000X.

Although these dewetted films show improved crystallinity in XRD (data not shown) over as-ED_ref CuInSe₂ films, they are not suitable for PV applications because any attempt to synthesize a PV device would result in shorting out of the cell. Thus we further made an attempt to work in submelting regime so as to avoid dewetting but at the same time reach high enough temperatures to drive atomic diffusion. Various CuInSe₂ films underwent PLA at 50, 60 and 70 mJ/cm². The number of laser pulses was also varied up to 1000 and frequency varied up to 400 Hz. Figure 3 (a) and (b) show the SEM images of as-ED_ref CuInSe₂ film and the film that underwent PLA at 70 mJ/cm² for 1000 pulses working at 400 Hz respectively. As can be seen from the Fig. 3(b) there is no sign of melting which justified our working at low fluence. However no improvements are seen in XRD results of the films. Figure 3(c) shows XRD θ -2 θ scan of as-ED CuInSe₂ film and films that underwent PLA at 70 mJ/cm² for 1000 pulses working at 10 and 400 Hz. The XRD θ -2 θ scan clearly show no improvement after PLA as is evident by broad XRD peaks.



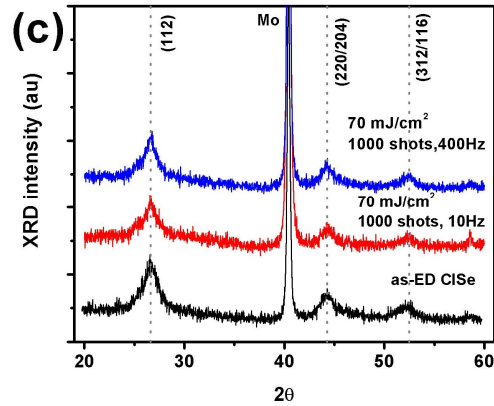


Figure 3. SEM images of (a) as-ED CuInSe₂ ref film, (b) PLA at 70 mJ/cm² for 1000 pulses at 400 Hz and (c) shows XRD scans of as-ED CuInSe₂ films and samples that underwent PLA at 70 mJ/cm² for 1000 pulses at 10 Hz and 400 Hz. The SEM images shown are at 5000X.

These results prompted us to think carefully about the PLA process. The atomic diffusion length ($2\sqrt{Dt}$, $D(T)$ = diffusion coefficient which is a function of temperature (T) and t = time of annealing) is the main idea behind the annealing theory of a material system. Now we realize that in order to increase atomic diffusion length i.e. to improve crystallinity of CuInSe₂ system we could either increase $D(T)$ or t . PLA has been used earlier to successfully synthesize metastable high quality epitaxial thin films of Ga_{1-x}Mn_xAs [14], Ga_{1-x}Mn_xP [15], Zn_{1-x}Mn_xTe_{1-y}O_y [16] and also polycrystalline Ge_xSn_{1-x} thin films [17]. For all these alloy systems the main principle behind epitaxial growth is that an amorphous layer on top of a epitaxial substrate is heated up to melting temperature ($D(T)$ is increased) within few ns time frame. Although the top of the thin amorphous film is at the melting temperature the thin film-substrate interface is approximately close to room temperature. This drives rapid solidification of the thin film with underlying substrate acting as the template for the recrystallizing layer. The melt wets the solid completely and epitaxial growth occurs.

In the case of electrodeposited CuInSe₂ on Mo (commonly used back contact), increasing T beyond T_{melt} results in dewetting of CuInSe₂. Electron back scatter diffraction (EBSD) data [7] revealed that dewetted CuInSe₂ droplets sit on top of Mo. These droplets have a amorphous shell with the recrystallized grains in the core. The amorphous shell could be overcome by using slower pulses, but the gathering up of the CuInSe₂ into droplets is a no-go and will be present, for any conditions producing a melt for long enough time for viscous flow to occur. If it is made faster so that the liquid solidified before droplet formation, then we face another problem of amorphous solidification. So we conclude that there is no process window at all, unless the interface energetics are changed. However as discussed earlier changing the substrate to Cu also did not solved the dewetting problem. Although there exists a possibility of trying out liquid phase CuInSe₂ recrystallization using other suitable back contact layers such as W, Ta etc. [18]. However even if successful, the implications of using a different back contact layer in terms of device performance would need to be tackled.

The other approach to increase crystallinity will be to work under the submelting regime ($T < T_{\text{melt}}$). As discussed earlier working in submelting regime also did not help us in improving crystallinity of the samples. This is because of the constraint imposed by t which is < 150 ns and is probably not large enough for long range diffusion. The reason behind this is simple to understand. The work frequency of our system is varied from 10 Hz to 400 Hz which is equivalent to 2.5 ms, about five orders of magnitude greater than the pulse width. This implies that the each pulse that CuInSe₂ film is exposed to (either 5 or 1000) is acting independently of each other resulting in non-effective diffusion. One of the possible but difficult way to counter this would be to work with a laser system which can possibly work at MHz and still deliver high energy laser pulses to drive atomic diffusion in submelting regime.

The other possibility that exists and we have used here on is to increase the annealing time by switching from PLA mode to CWLA mode. The advantage that CWLA mode offers over PLA mode is that it helps in maintaining steady state temperature of the sample higher than PLA for longer time. Although PLA gives us a burst of photons resulting in high peak power, it is not able to drive long range atomic diffusion. What we need is energy distribution over a long interval of time, long enough to drive atomic diffusion and at the same time low enough to avoid melting of CuInSe₂ film. We would like to point out here that by long range diffusion we simply mean an annealing process which gives us an

increase in X-ray coherence length by about 10 times i.e. approximately from 7 nm to 70 nm. These estimates are based on Scherrer's formula [19] applied to EDA_ref and furnace annealed CISE [20-21] samples respectively.

3.2 Continuous wave laser annealing (CWLA) using 1064 nm laser

Based on different experiments conducted with CWLA of CuInSe₂ films using 1064 nm laser, we found that a power density of 50 W/cm² is a good starting point for investigations. Figure 4(a) shows XRD θ -2 θ scan of as-ED CuInSe₂ film and films that underwent CWLA processing for varying times. The as-electrodeposited CuInSe₂ film (reference sample) is in the form of nano-crystallites which causes a broad θ -2 θ diffraction peaks (Fig.4(b)). After CWLA processing, all of the XRD peaks i.e. (112), (220/204) and (312/116) become both narrow and intense indicating improved intragranular crystalline quality and or grain growth. There is more than 80% reduction in full width at half maximum (FWHM) of the XRD peaks after CWLA (Fig. 4(b)). The FWHM of the XRD peaks (Fig.4(b)) after CWLA is comparable to what we have observed by annealing these as-ED CuInSe₂ films by furnace annealing [20-21] or rapid thermal annealing [22-23]. However the main difference is the timescale of annealing. The CWLA is about 100 times faster than furnace annealing and 10 times faster than the time at the highest temperature in RTA. Also there is no signature of any other secondary phase evident in the XRD measurements.

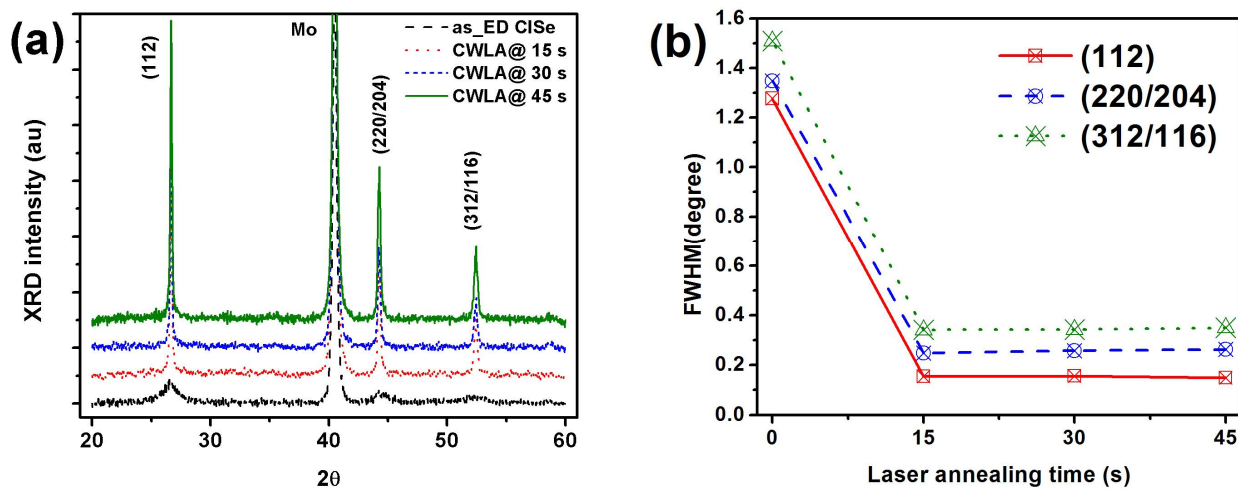


Figure 4. (a) XRD θ -2 θ scan of as-ED CuInSe₂ film and CWLA samples for varying annealing time and (b) Change in FWHM values of XRD peaks for varying annealing time.

The as-ED_ref CuInSe₂ samples appear dark grey, and after CWLA the color of the film changes to light grey. The SEM images (Fig.5 (a) and (b)) of the samples further confirmed that the power density is low enough to avoid even surface melting and thus dewetting. The lack of apparent change in surface morphology is consistent with the results of furnace annealed samples. [5] EDS measurements of the samples suggest that all of the samples are Cu-rich (Cu/In>1) (Fig.5(c)) however after KCN etching all of the CWLA samples become Cu-poor (Fig.5(c)). The Cu-poor composition is known to promote the formation of an ordered defect phase such as CuIn₃Se₅ which result in lower interface recombination in solar cells. The observation of a Cu-poor composition suggests that Cu diffuses into the film, as it is known that In_xSe_y compounds are more volatile [24]. We also observe that the sampled volume becomes progressively Se-poor as the CWLA time increases (Fig.5(c)). This will pose a challenge for incorporation of CWLA in making photovoltaic devices as Se vacancies are known to severely restrict cell efficiency. Incorporation of additional processes or the modification of the laser step will be critical for use of CWLA in actual cell processing.

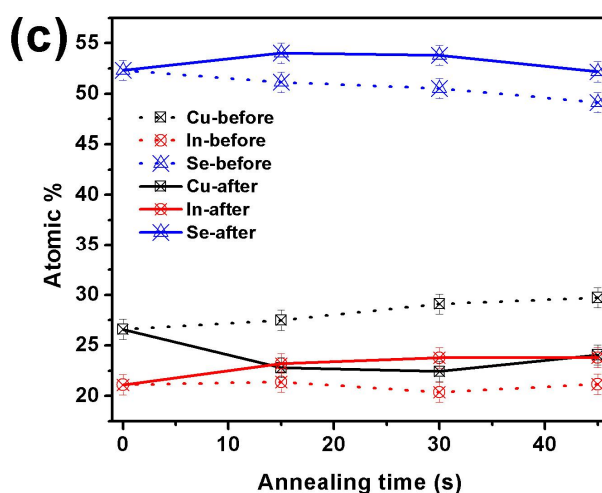
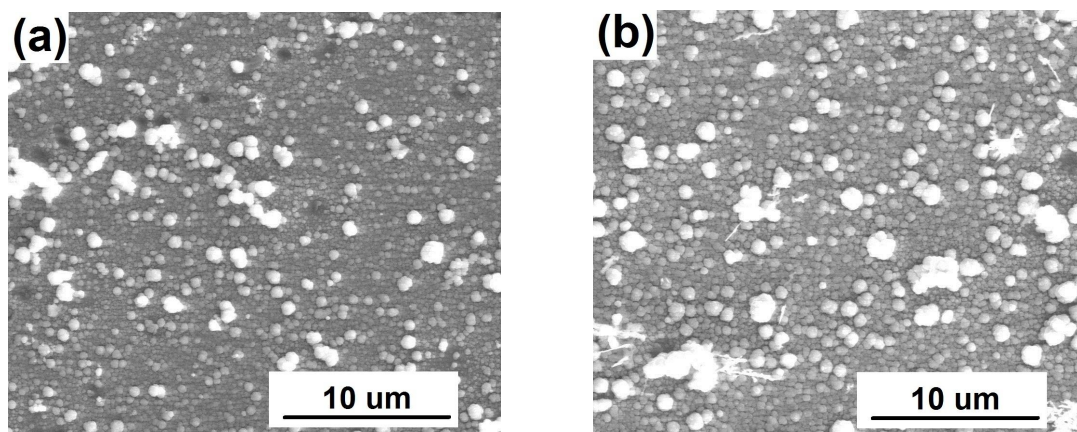


Figure 5. SEM image of (a) as-ED CuInSe₂ film, (b) CuInSe₂ film after 45 s annealing and (c) shows the EDS measurements of the samples before (dotted line) and after (solid line) KCN etching. The SEM images shown are at 10000X.

In order to confirm the correct phase formation, Raman spectroscopy was performed on the CWLA samples. While XRD gives information about the bulk of the film, by carefully choosing the excitation wavelength depth analysis of the films could be performed by using Raman spectroscopy. The position of Raman peaks gives information about the phases present and shape of peak in Raman spectrum can give information about the order and or disorder state of the material. Also Raman spectroscopy is an important tool for characterization of chalcopyrite thin films as against XRD because XRD peaks of phases such as sphalerite, Cu_xSe_y etc. lie close to XRD peaks of the chalcopyrite phase of CuInSe₂ thus making the analysis difficult or even misinterpretation of the data. Raman spectrum is useful in the sense that it can clearly distinguish between the phase present. Figure 6(a) shows the Raman spectra of as-ED_ref and the laser annealed samples in the spectral range of 125-300 cm⁻¹. We observe no peaks besides those attributable to CuInSe₂ in the Raman studies. Single crystalline CuInSe₂ has a dominant Raman peak at 174-175 cm⁻¹ corresponding to the chalcopyrite (CH) A₁ vibration mode. [25] This mode corresponds to motion of all of the Se anions against the cation sublattice. The other phonon mode that is generally seen in the Raman spectrum of CuInSe₂ is a mixed B₂-E mode observed around 220 cm⁻¹. [25]

The Raman spectrum for the as-ED_ref sample (Fig.6(a)) is featureless except for a broad hump extending from 150 to 250 cm⁻¹ indicating high disorder in the as-ED state. However after CWLA both A₁ and mixed B₂-E modes emerge indicating increased crystalline quality. As the laser annealing time increases the position of the A₁ mode (Fig.6(b)) approaches close to 176 cm⁻¹, as is seen for ED furnace annealed samples also[20-21]. The small shift of the A₁ mode

towards higher wavenumber has been attributed to compressive stress [26] or to the presence of extended defects such as twins, dislocations and grain boundaries [27]. Similar to the XRD results, increased CW annealing time, decreases the FWHM of the Raman A_1 mode by more than 80%. The FWHM of the A_1 mode ($\approx 12 \text{ cm}^{-1}$) for CWLA films is comparable to furnace annealed samples.[20-21].

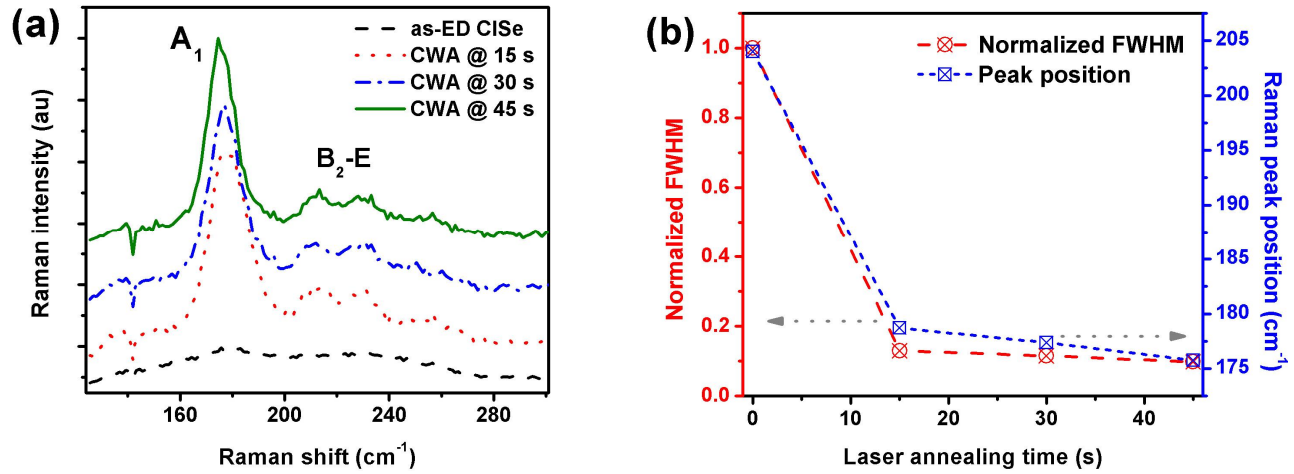


Figure 6. (a) Raman spectrum of as-ED_ref CuInSe₂ film and all CWLA samples and (b) shows variation in FWHM and A_1 mode peak position as the annealing time is varied.

CONCLUSIONS

In summary we have investigated pulsed laser annealing (PLA) and continuous wave laser annealing (CWLA) using a 1064 nm laser with 75-150 ns pulse duration on as-ED CuInSe₂ films. PLA results indicate that at high fluence ($\geq 100 \text{ mJ/cm}^2$) CuInSe₂ films melt and dewet on both Mo and Cu substrates. In the submelting regime ($\leq 70 \text{ mJ/cm}^2$) no change is seen in crystalline quality using XRD. Thus we conclude that no PLA processing window for structural modification of CuInSe₂ absorber films exists for lasers with similar parameters. However 1064 nm CWLA at 50 W/cm^2 for $\geq 15 \text{ s}$ results in dramatically improved crystalline quality without even surface melting, showing that all changes occur in the solid phase. Raman analysis indicates the formation of the chalcopyrite phase with structural quality very similar to that obtained by furnace annealing; both XRD and Raman show $\geq 80\%$ reduction in FWHM for their respective primary peaks. EDS measurements however indicate decrease in Se content with increasing laser annealing time. We are working towards optimizing our laser annealing process so as to minimize the laser annealing time, implement CWLA on 1 μm CISE films and minimize Se loss from the films. We hope that these preliminary results using CWLA will help in setting the platform for our long term goal of implementing laser annealing for CIGS processing at industrial scale level.

ACKNOWLEDGEMENTS

The work at the University of Utah was fully supported by the US National Science Foundation under the Materials World Network program award 1008302 and the work at University of Luxembourg was fully supported by Fonds National de la Recherche du Luxembourg grant MAT09/02. The authors would like to thank M.A. Karmarkar for help in carrying out the Raman measurements.

REFERENCES

- [1] Green, M.A., Emery, K., Hishikawa, Y., Warta, w., and Dunlop, E.D., "Solar cell efficiency tables (version 39)", *Prog. Photovolt: Res. Appl.*, 20(1) 12-20 (2012).
- [2] Jackson, P., Hariskos, D., Lotter, E., Paetel, S., Wuerz, R., Menner, R., Wischmann, W., and Powalla, M., "New world record efficiency for Cu(In,Ga)Se₂ thin-film solar cells beyond 20%", *Prog. Photovolt: Res. Appl.* 19(7) 894-897 (2011).
- [3] Voß, T., Schulze, J., Kirbs, A., Palm, J., Probst, V., Jost, S., Hock, R., Purwins, M., "CIS solar cells by high rate electrodeposition technology", *Proceedings of the 22nd European Photovoltaic Solar Energy Conference and Exhibition, Sep. 3 - 7, 2007, Milan (Italy)*.
- [4] http://www.electrochem.org/dl/interface/sum/sum11/sum11_p047-053.pdf, July 10, 2012.
- [5] Dale, P.J., Samantilleke, A. P., Zoppi, G., Forbes, I. and Peter, L. M., "Characterization of CuInSe₂ material and devices: comparison of thermal and electrochemically prepared absorber layers", *J. Phys. D: Appl. Phys.* 41 (2008), 085105
- [6] Meyer, J. R., Bartoli, F. J. and Kruer, M. R., "Optical heating in semiconductors", *Phys. Rev. B*, 21(4), 1559, (1980).
- [7] Bhatia, A., Dale, P.J., Nowell, M.M., and Scarpulla, M.A., "Pulsed Laser Processing of Electrodeposited CuInSe₂ Photovoltaic absorber thin films", *Mat. Res. Soc. Symp. Proc.* 1268 EE4.10 (2010)
- [8] Bhatia, A., Meadows, H., Hlaing Oo, W.M., Dale, P.J., and Scarpulla, M.A., " Pulsed Laser Processing of Electrodeposited CuInSe₂ Photovoltaic Absorber Thin Films", *Conference record of the 37th IEEE Photovoltaic Specialists Conference (2011)*, DOI: 10.1109/PVSC.2011.6185931
- [9] Jost,S., Schurr, R., Hergert, F., Hock, R., Schulze, J., Kirbs, A., Voß, T., Purwins, M., Palm, J. and Mys, I., " The formation of CuInSe₂ thin-film solar cell absorbers by laser annealing of electrodeposited precursors", *Sol Energ Mat Sol C*, 92, 410, (2008)
- [10] Joliet, M.C., Antoniadis, C., Andrew, R., and Laude, L.D., "Laser induced synthesis of thin CuInSe₂ films", *Appl. Phys. Lett.* 46(3), (1985) 266-267
- [11] Joliet, M.C., Antoniadis, C., Andrew, R., and Laude, L.D., "Laser induced synthesis of thin CuInSe₂ films", *Thin solid films*, 126(3), (1985) 143-148
- [12] Mooney, G.D. and Hermann, A.M., *Energy Res. Abstr.* 15 (23) (1990) (Abstr. no. 50720).
- [13] Mooney, G.D. and Hermann, A.M., *Energy Res. Abstr.* 14 (21) (1989) (Abstr. no. 44906).
- [14] Scarpulla, M. A., Dubon, O. D., Yu, K. M., Monteiro, O., Pillai, M. R., Aziz, M. J., and Ridgway, M. C., "Ferromagnetic Ga_{1-x}Mn_xAs produced by ion implantation and pulsed-laser melting", *Appl. Phys. Lett.*, 82(8):1251-1253 (2003)
- [15] Scarpulla, M. A., Cardozo, B. L., Farshchi, R., Hlaing, W. M., McCluskey, M. D., Yu, K. M., and Dubon, O. D., " Ferromagnetism in Ga_{1-x}Mn_xP: Evidence for Inter-Mn Exchange Mediated by Localized Holes within a Detached Impurity Band", *Phys. Rev. Lett*, 95: 207204 (2005)
- [16] Yu, K. M., Walukiewicz, W., Wu, J., Shan, W., Beeman, J. W., Scarpulla, M. A., Dubon, O. D., and Becla, P., " Diluted II-VI Oxide Semiconductors with Multiple Band Gaps", *Phys. Rev. Lett*, 91(24): 246403 (2003)
- [17] Bhatia, A., Hlaing Oo, W.M., Siegel, G., Stone, P.R. Yu, K.M. and Scarpulla, M.A., "Ion Implantation & Pulsed Laser Melting (II-PLM) Synthesis of Epitaxial Ge_{1-x}Sn_x Alloy Thin Films", *J. Electronic Materials*, 41(5) 837-844 (2012)
- [18] Orgassa, K., Schock, H.W. and Werner, J.H., "Alternative back contact materials for thin film Cu(In,Ga)Se₂ solar cells", *Thin solid films*, 126(3), (1985) 143-148
- [19] Suryanarayana, C. and Norton, M.G., [X-Ray diffraction: A practical approach], Springer (1998)
- [20] Bhatia, A., Meadows, H., Hlaing Oo, W.M., Dale, P.J. and Scarpulla, M.A., Effects of pulsed laser annealing (PLA) on deep level defect populations in electrochemically-deposited and annealed CuInSe₂ thin films, Under Review
- [21] Bhatia, A., Meadows, H., Hymas, M.C., Smith, E.M., Dale, P.J. and Scarpulla, M.A., "Study of point defects in ns pulsed-laser annealed CuInSe₂ thin films" *Conference record of the 38th IEEE Photovoltaic Specialists Conference (2012)*
- [22] Bhatia, A., Karmarkar, Meadows, H.M., A., Dale, P.J., and Scarpulla, M.A., "Grain growth study of electrochemically deposited CuInSe₂ by rapid thermal annealing in sulfur atmosphere", *Proceedings of the SPIE XVI International Workshop on the Physics of Semiconductor Devices, PV19 (2012)*, In press

- [23] Bhatia, A., Karmarkar, Meadows, H.M., Hymas, M.C., Smith, E.M., Dale, P.J. and Scarpulla, M.A., " Effects of annealing in sulfur vapor on electrodeposited CuInSe₂ films", Conference record of the 38th IEEE Photovoltaic Specialists Conference (2012)
- [24] Scheer, R. and Schock, H.W., [Chalcogenide Photovoltaics physics, technologies, and thin film devices], Weinheim, Germany : Wiley-VCH, (2011)
- [25] Rincon, C. and Ramirez, F.J., "Lattice vibrations of CuInSe₂ and CuGaSe₂ by Raman microspectrometry", J. Appl. Phys., 72 (9), 4321, (1992).
- [26] Ramdani, O., Guillemoles, J.F., Lincot, D., Grand, P.P., Chassaing, E., Kerrec, O., Rzepka, E., "One-step electrodeposited CuInSe₂ thin films studied by Raman spectroscopy", Thin solid films, 515, (2007) 5909-5912.
- [27] Izquierdo-Roca, V., Alvarez-García, J., Calvo-Barrio, L., Pérez-Rodríguez, A., Morante, J. R., Bermudez, V., Ramdani, O., Grand, P.-P. and Kerre, O., "Raman scattering characterisation of electrochemical growth of CuInSe₂ nanocrystalline thin films for photovoltaic applications: Surface and in-depth analysis", Surf. Interface Anal. (2008); 40: 798–801.